Cosmic Constraint to DGP Brane Model: Geometrical and Dynamical Perspectives

Lixin Xu*† and Yuting Wang
Institute of Theoretical Physics, School of Physics & Optoelectronic Technology, Dalian University of Technology, Dalian, 116024, P. R. China

In this paper, the Dvali-Gabadadze-Porrati (DGP) brane model is confronted by current cosmic observational data sets from geometrical and dynamical perspectives. On the geometrical side, the recent released Union2 557 of type Ia supernovae (SN Ia), the baryon acoustic oscillation (BAO) from Sloan Digital Sky Survey and the Two Degree Galaxy Redshift Survey (transverse and radial to line-of-sight data points), the cosmic microwave background (CMB) measurement given by the seven-year Wilkinson Microwave Anisotropy Probe observations (shift parameters R, $l_a(z_*)$ and redshift at the last scatter surface z_*), ages of high redshifts galaxies, i.e. the lookback time (LT) and the high redshift Gamma Ray Bursts (GRBs) are used. On the dynamical side, data points about the growth function (GF) of matter linear perturbations are used. Using the same data sets combination, we also constrain the flat ΛCDM model as a comparison. The results show that current geometrical and dynamical observational data sets much favor flat ΛCDM model and the departure from it is above $4\sigma(6\sigma)$ for spatially flat DGP model with(without) SN systematic errors. The consistence of growth function data points is checked in terms of relative departure of redshift-distance relation.

PACS numbers: 98.80.Es, 04.50.-h, 04.50.Kd, 95.36.+x

I. INTRODUCTION

Understanding the current accelerated expansion of our universe has become one of the most important issues of modern cosmology [1, 2]. However, as so far, we still know little about the nature of current accelerated expansion. In general, from the phenomenological points of view, the possible models can be classified by the form of Friedmann equation. One is

$$H^2 = f(\rho), \tag{1}$$

where the extra energy component(s) is(are) added on the right hand of Einstein's equations, and $f(\rho)$ is a function of energy density ρ which can be composed from dark matter and extra energy components. Here H is the Hubble parameter. The other is

$$g(H^2) = \rho, \tag{2}$$

where the energy component(s) is (are) invariant and the *Gravity Theory* or equivalently the relation of Hubble parameter H with the conventional matter (dark matter at late time) can be altered, $g(H^2)$ is a function of H^2 or H. For recent reviews about dark energy and an accelerated expansion universe, please see [3].

In this paper, we will consider a leading modified gravity model, Dvali-Gabadadze-Porrati (DGP) brane model [4], for the review, please see [5]. In DGP brane model, a tensionless four-dimensional brane (a hypersurface with a vanishing cosmological constant) is embedded in a five dimensional bulk which is a flat Minkowski space-time, where the gauge forces are confined on the brane and gravity can propagate in all dimensions freely. Below the crossover scale r_c, the gravity appears four-dimensional. However, above the scale r_c the gravity can leak into the extra dimension and make the conventional four-dimensional gravity altered. It is due to the leakage of gravity, the current universe appears an accelerated expansion phase.

In the past years, the DGP model has been constrained by cosmic observational data sets, for recent constrained results, please see [6] in geometrical side and [7] in dynamical side. Importantly, Lombriser *et.al.* [8] constrained DGP brane model exhaustively by adopting a parameterized post-Friedmann description of gravity, where all of the CMB data, including the largest scales, and its correlation with galaxies in addition to the geometrical constraints from supernovae distances and the Hubble constant were utilized. Of course, it is more important and necessary to constrain

* Corresponding author
†Electronic address: lxxu@dlut.edu.cn

a cosmological model by using all of CMB data and its correlation with large scale structure, say galaxy. However, it is much complicated when we have to resort to some kinds of Boltzmann-codes, say the famous **CMBfast** and **CAMB**. It would be interesting, if this complication is avoided, and a relative stronger prediction is arrived. In this paper, we will investigate this kind of possibility by combining the geometrical and dynamical perspectives without the above mentioned complication. Via this combination, the constraint becomes much tight and efficient because it relies on both gravity theory and background geometry. On the geometrical side, we will consider the luminosity-distance relation of SN and GRB, the standard rulers from BAO, x-ray gas fraction and CMB, also the lookback time of high redshift galaxy. For the dynamical perspective, we mainly consider the growth function $\delta(z) \equiv \frac{\delta\rho}{\rho}(z)$ of the linear matter density contrast as a function of redshift. As well known, the data points of growth function were obtained with the help of ΛCDM model and the reliability will be reduced when it is used to constrain other cosmological models, however this problem can be evaded in the DGP model if it has similar expansion history to that of ΛCDM [7, 9]. In fact, the use of redshift-distance relation of ΛCDM (with $\Omega_m = 0.25$ for the data point at $z = 0.77$ and $\Omega_m = 0.30$ for the remained five data points) makes the the data points of growth function weak to constrain other cosmological model [10]. In [9], to use these data points to find the growth index of DGP model, the DGP model parameters were selected properly to make redshift-distance relation be the same as that of ΛCDM model. In fact, we can firstly neglect this weak point and just use these data points as dynamical constraint beyond ΛCDM model. After it was done, we can check the consistence via investigating the possible departure from ΛCDM model with the best fit values of model parameters. If the departure is large, the data points must be discarded and the data fitting is not reliable. In fact, one will find that the redshift-distance relations of ΛCDM and DGP model are almost the same and the relative departure from ΛCDM model is up to 10% in terms of $H_0 r(z)$ when Ω_m varies in the range $[0.28, 0.32]$, where $\Omega_m = 0.30$ is fixed in ΛCDM model. When the values of Ω_m increase, the relative departure becomes small. And the departure is smaller than the errors of growth function data points. Based on this point, the data points of growth function can be used safely to constrain DGP model. Also, when the data points of growth function are used to confront other cosmological models, the consistence must be checked.

For the DGP model, the modified Friedmann equation is given as [11]

$$H^2 + \frac{k}{a^2} = \left[\sqrt{\frac{\rho}{3M_{pl}^2} + \frac{1}{4r_c^2}} + \frac{1}{2r_c}\right]^2 \tag{3}$$

where $r_c = M_{pl}^2/2M_5^3$ is the so-called crossover scale, M_{pl} and M_5 are four- and five-dimensional reduced Planck mass respectively, ρ is the cosmological fluid which includes conventional matter contents and radiation, $k = 0, \pm 1$ is three dimensional spatial curvature factor. In terms of the dimensionless density parameters, the Friedmann equation can be rewritten as

$$E^2(z) = \Omega_k(1+z)^2 + \left(\sqrt{\Omega_m(1+z)^3 + \Omega_r(1+z)^4 + \Omega_{r_c}} + \sqrt{\Omega_{r_c}}\right)^2, \tag{4}$$

where $E^2(z) = H^2(z)/H_0^2$ and $\Omega_{r_c} = 1/(4r_c^2H_0^2)$ is a constant which respects to the constraint equation

$$\Omega_k + \left(\sqrt{\Omega_m + \Omega_r + \Omega_{r_c}} + \sqrt{\Omega_{r_c}}\right)^2 = 1. \tag{5}$$

For the spatially flat case ($\Omega_k = 0$), the above equation reduces to $\Omega_{r_c} = (1 - \Omega_m - \Omega_r)^2/4$.

II. METHOD AND RESULTS

In our calculations, we have taken the total likelihood function $L \propto e^{-\chi^2/2}$ to be the products of the separate likelihoods of SN (with and without systematic errors), BAO, CMB, GRBs, CBF, LT and GF. Then we get χ^2

$$\chi^2 = \chi^2_{SN} + \chi^2_{BAO} + \chi^2_{CMB} + \chi^2_{GRBs} + \chi^2_{CBF} + \chi^2_{LT} + \chi^2_{GF}, \tag{6}$$

where the separate likelihoods of SN, BAO, CMB, GRBs, CBF, LT, GF and the current observational datasets used in this paper are shown in the Appendix A.

In our analysis, we perform a global fitting to determine the cosmological parameters using the Markov Chain Monte Carlo (MCMC) method. The MCMC method is based on the publicly available **CosmoMC** package [12] and the **modified CosmoMC** package [13–15], including the X-ray cluster gas mass fraction. For our models we have modified these packages to add some subroutines, for example the code calculating the growth function likelihood etc. The following basic cosmological parameters ($\Omega_b h^2$, $\Omega_c h^2$) are varying with top-hat priors: the physical baryon

Datasets	Parameters	χ^2_{min}/d.o.f	Ω_m	H_0
GF5	9	697.342/645	$0.265^{+0.0291}_{-0.0302}$	$65.219^{+2.190}_{-1.956}$
GF6	9	707.750/646	$0.266^{+0.0298}_{-0.0304}$	$65.0873^{+2.413}_{-1.985}$
GF5(SN Sys.)	9	663.561/645	$0.285^{+0.0470}_{-0.0286}$	$63.754^{+2.142}_{-2.575}$
GF6(SN Sys.)	9	673.641/646	$0.297^{+0.0367}_{-0.0391}$	$63.121^{+2.629}_{-2.0471}$

TABLE I: The results of χ^2_{min}, Ω_m and H_0 with 1σ regions are listed. GF5 denotes 5 growth function data points are used without $z = 3.0$ data point. And, GF6 denotes the corresponding 6 data points case. SN Sys. denotes the results with SN systematic errors. d.o.f denotes the degrees of freedom.

Datasets	Parameters	χ^2_{min}/d.o.f	Ω_m	H_0	Ω_k
non-flat	10	684.251/644	$0.270^{+0.0278}_{-0.0323}$	$66.798^{+2.85}_{-2.483}$	$0.0123^{+0.00789}_{-0.00993}$
non-flat(SN Sys.)	10	647.543/644	$0.295^{+0.0419}_{-0.0345}$	$65.519^{+2.490}_{-2.974}$	$0.0153^{+0.00777}_{-0.01052}$

TABLE II: The results of χ^2_{min}, Ω_m, H_0 and Ω_k without $z = 3.0$ data point in non-flat DGP model. SN Sys. denotes the results with SN systematic errors. d.o.f denotes the degrees of freedom.

density $\Omega_b h^2 \in [0.005, 0.1]$, the physical dark matter energy density $\Omega_c h^2 \in [0.01, 0.99]$. And, in the data fitting process another seven parameters $(K, \eta, \gamma, b_0, \alpha_b, s_0, \alpha_s)$ included in the X-ray gas mass fraction f_{gas} are treated as free parameters. As a byproduct the best fitting values of these parameters are obtained. And, these values can also be taken accounted as a check of data fitting.

From the observational results listed in Tab. VII, one has noticed that the datum at $z = 3.0$ is odd in some degree for its value is above 1. So in data fitting process, we have considered two cases with and without inclusion of $z = 3.0$ data point. The constrained results are shown in Tab. I and Fig. 1 (with SN systematic errors). From Tab. I, one can easily see that the value of χ^2_{min} is smaller and the constraint is tighter without $z = 3.0$ data point than that with it. Under this status, one would constrain a cosmological model without the inclusion of $z = 3.0$ data point. For the non-flat DGP model, we summarize the model parameters values in Tab. II and Fig. 2 (with SN systematic errors). As a comparison, using the same combination (with SN systematic errors) to the flat ΛCDM model, we have the results $\chi^2_{min} = 626.057$, $\Omega_m = 0.281^{+0.0300}_{-0.0360}$ and $H_0 = 69.658^{+3.0176}_{-2.142}$. One can see that the best fit values of Ω_m and 1σ errors of model parameters are enlarged when SN systematic errors are included. As contrasts, the current Hubble values and χ^2_{min} are lower in the case of SN systematic errors included.

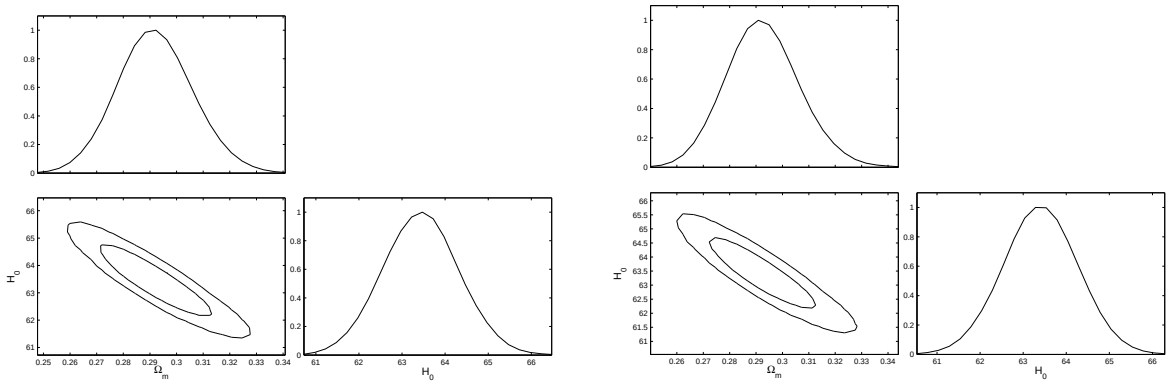

FIG. 1: The 2-D contours with 1σ, 2σ regions and 1-D marginalized distribution of Ω_m, H_0. Left Panel: $\chi^2_{min} = 663.561$, $\Omega_m = 0.285^{+0.0470}_{-0.0286}$ and $H_0 = 63.754^{+2.142}_{-2.575}$ with 5 growth function data points, $z = 3.0$ is removed. Right Panel: $\chi^2_{min} = 673.641$, $\Omega_m = 0.297^{+0.0367}_{-0.0391}$ and $H_0 = 63.121^{+2.629}_{-2.0471}$ with all 6 growth function data points included.

Now, it's time to check the consistence of our treatment of the points of growth function. We calculate the relative departure of comoving distance

$$\text{rel.dep.} = \frac{r_{DGP}(z) - r_{\Lambda CDM}(z)}{r_{\Lambda CDM}(z)} \tag{7}$$

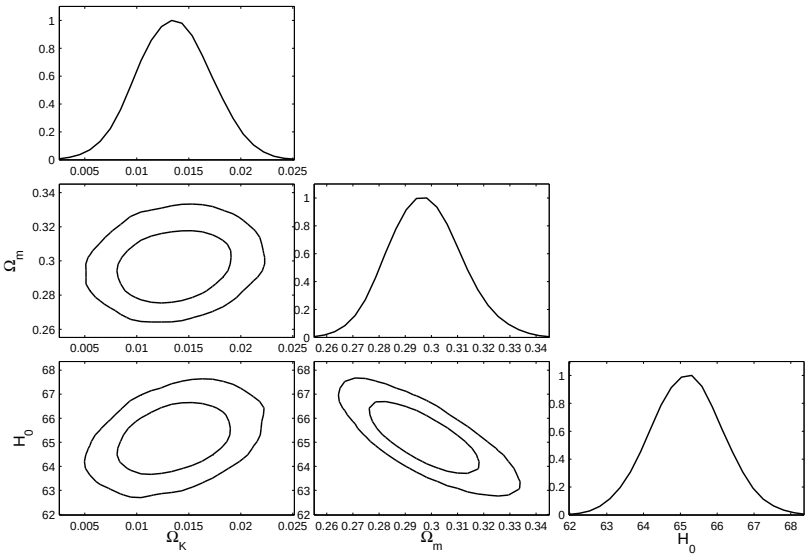

FIG. 2: The 2-D contours with 1σ, 2σ regions and 1-D marginalized distribution of Ω_m, H_0 and Ω_k in non-flat DGP model without $z = 3.0$ data point.

where $\Omega_m = 0.30$ is fixed in ΛCDM model. The result is shown in Fig. 3. In fact, one can check the consistence via the relative departure in terms $H_0 r(z)/c$ with the variables of z and Ω_m, the corresponding result is shown in a 3D plot, see Fig. 4. Clearly, the relative departures are up to 10% for neglecting the uncertainty of H_0. And, with the increasing value of Ω_m, the departure is amplifying. In fact, as shown in Fig. 3, the departure is just up to 8% when the best fit values of model parameters are adopted.

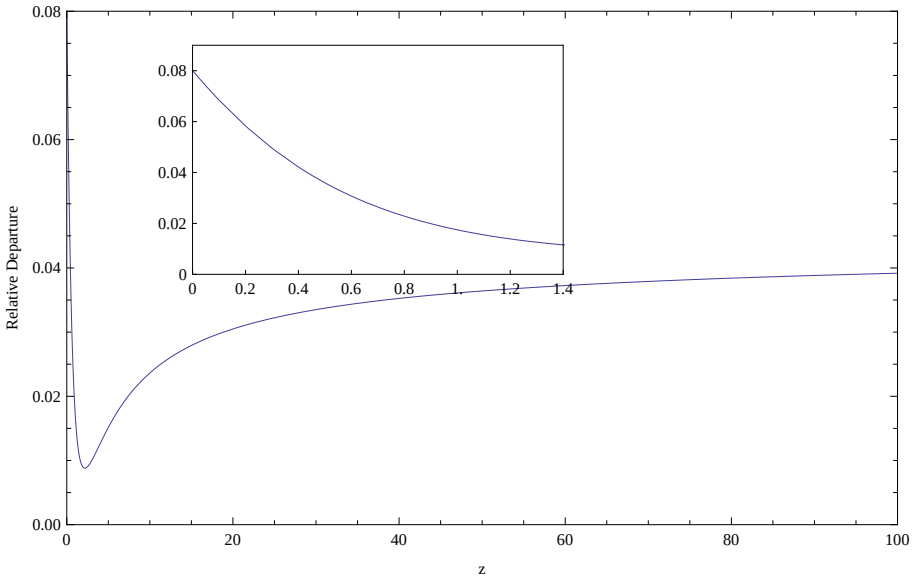

FIG. 3: The relative departure of redshift-distance $r(z)$ of DGP model with the best fit values of model parameters from ΛCDM model with $\Omega_m = 0.30$ and $H_0 = 69.658$.

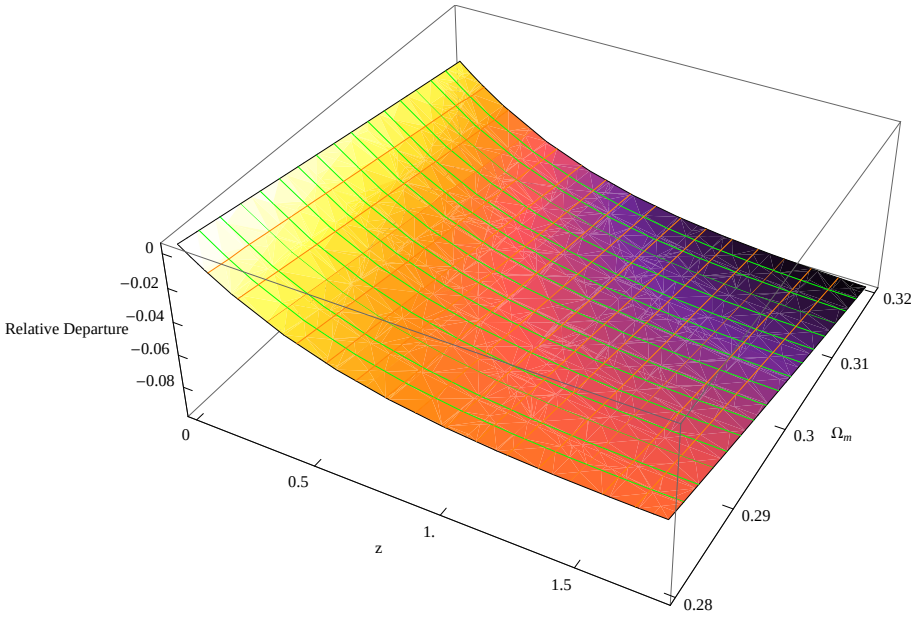

FIG. 4: The relative departure of redshift-distance in terms of $H_0 r(z)$ of DGP model from ΛCDM model with redshift and Ω_m where $\Omega_m = 0.3$ is fixed in ΛCDM model.

III. CONCLUSION AND DISCUSSION

In summary, in this paper we have performed a global fitting on the cosmological parameters in both the flat DGP model and the non-flat DGP model by using a completely consistent analysis from the geometrical and dynamical perspectives. On the geometrical side, the X-ray gas mass fraction observation, type Ia supernovae data from Union2 set, transverse and radial baryon acoustic oscillations data from SDSS, the measurement data on current Cosmic Microwave Background from the seven-year WMAP observations, the lookback time data derived from the ages of galaxy and clusters and the high redshift gamma ray bursts. On the dynamical side, the data points about the growth function of matter linear perturbations are included. The constrained results are shown in Tab. I for the flat case and Tab. II for the non-flat case. The results show that the $z = 3.0$ data point of growth function is odd in some degrees. So, in the future work when the observational growth function data points are used as cosmic constraint, this point would be removed. As a comparison, using the same data points combination, the flat ΛCDM model was constrained, where we have $\chi^2_{min} = 626.057$, $\Omega_m = 0.281^{+0.0300}_{-0.0360}$ and $H_0 = 69.658^{+3.0176}_{-2.142}$. Clearly, one can easily find that $\Delta\chi^2 = 37.504$ which in terms of σ distance is 4.25 for 9 parameters via the formula $1-\Gamma(\nu/2, \Delta\chi^2/2)/\Gamma(\nu/2) = \mathrm{Erf}(d_\sigma/\sqrt{2})$, where $\nu = 9$ is the number of free model parameters. It means that current geometrical and dynamical observational data sets favor flat ΛCDM model more above 4σ than that for spatially flat DGP model. This conclusion is consistent and comparable with that of [8]. When the same process of data fitting is implemented without SN systematic errors, the departure from ΛCDM model can be improved to about 6σ for the flat DGP model. To check the consistence of growth function data points, the relative departure of DGP model with best fit model parameters from ΛCDM model with fixed $\Omega = 0.30$ is up to 8%. In general, the relative departure in terms of $H_0 r(z)$ is up to 10% when Ω_m varies in the range $[0.28, 0.32]$ and $\Omega_m = 0.30$ is fixed in ΛCDM model. With this observation, we can say that growth function data points can be used to constrain DGP model. So far, we have seen that it is possible to give some strong prediction without having to resort to the complicated modification of the Boltzmann-codes. At least, for flat DGP model, it is possible. It is because that the discrepancy will be enlarged when more observational data points are included. We expect this work can shed light on distinguish dark energy models. At last, we are pleasant to give some comments on the growth function data points used to constrain other cosmological models. The key point is the dependence of distance-redshift relation of spatially flat ΛCDM model with fixed value of $\Omega_m = 0.30$. Of course, one can firstly neglect this fact and do data fitting as what we have done in this paper. Then, one has to check the consistence. In fact, we can get around this problem in a different way. It is the full consideration of distance-redshift relation and introduction of some kinds of uncertainties in terms of redshift and growth function data points, put in another words, via the possible introduction of extra errors on redshifts and growth function data points. Of course, it is out the range of this paper. In the future work, this possibility will be researched.

Acknowledgments

This work is supported by NSF (10703001), SRFDP (20070141034) of P.R. China. We thank Prof. Deepak Jain and Dr. Yun Chen for the correspondence on lookback time data set. We appreciate the anonymous referee's invaluable help to improve this work.

Appendix A: Cosmological Constraints Methods

1. Type Ia Supernovae constraints

Recently, SCP (Supernova Cosmology Project) collaboration released their Union2 dataset which consists of 557 SN Ia [16]. The distance modulus $\mu(z)$ is defined as

$$\mu_{th}(z) = 5\log_{10}[\bar{d}_L(z)] + \mu_0, \tag{A1}$$

where $\bar{d}_L(z)$ is the Hubble-free luminosity distance $H_0 d_L(z)/c = H_0 d_A(z)(1+z)^2/c$, with H_0 the Hubble constant, defined through the re-normalized quantity h as $H_0 = 100h$ km s^{-1}Mpc^{-1}, and $\mu_0 \equiv 42.38 - 5\log_{10} h$. Where $d_L(z)$ is defined as

$$d_L(z) = (1+z)r(z), \quad r(z) = \frac{c}{H_0\sqrt{|\Omega_k|}}\text{sinn}\left[\sqrt{|\Omega_k|}\int_0^z \frac{dz'}{E(z')}\right] \tag{A2}$$

where $E^2(z) = H^2(z)/H_0^2$. Additionally, the observed distance moduli $\mu_{obs}(z_i)$ of SN Ia at z_i is

$$\mu_{obs}(z_i) = m_{obs}(z_i) - M, \tag{A3}$$

where M is their absolute magnitudes.

For the SN Ia dataset, the best fit values of the parameters p_s can be determined by a likelihood analysis, based on the calculation of

$$\begin{aligned}\chi^2(p_s, M') &\equiv \sum_{SN} \frac{\{\mu_{obs}(z_i) - \mu_{th}(p_s, z_i)\}^2}{\sigma_i^2} \\ &= \sum_{SN} \frac{\left\{5\log_{10}[\bar{d}_L(p_s, z_i)] - m_{obs}(z_i) + M'\right\}^2}{\sigma_i^2},\end{aligned} \tag{A4}$$

where $M' \equiv \mu_0 + M$ is a nuisance parameter which includes the absolute magnitude and the parameter h. The nuisance parameter M' can be marginalized over analytically [17] as

$$\bar{\chi}^2(p_s) = -2\ln\int_{-\infty}^{+\infty}\exp\left[-\frac{1}{2}\chi^2(p_s, M')\right]dM',$$

resulting to

$$\bar{\chi}^2 = A - \frac{B^2}{C} + \ln\left(\frac{C}{2\pi}\right), \tag{A5}$$

with

$$\begin{aligned}A &= \sum_i^{SN} \frac{\left\{5\log_{10}[\bar{d}_L(p_s, z_i)] - m_{obs}(z_i)\right\}^2}{\sigma_i^2}, \\ B &= \sum_i^{SN} \frac{5\log_{10}[\bar{d}_L(p_s, z_i)] - m_{obs}(z_i)}{\sigma_i^2}, \\ C &= \sum_i^{SN} \frac{1}{\sigma_i^2}.\end{aligned} \tag{A6}$$

Relation (A4) has a minimum at the nuisance parameter value $M' = B/C$, which contains information of the values of h and M. Therefore, one can extract the values of h and M provided the knowledge of one of them. Finally, note that the expression

$$\chi^2_{SN}(p_s, B/C) = A - (B^2/C), \tag{A7}$$

which coincides to Eq. (A5) up to a constant, is often used in the likelihood analysis [17, 18], and thus in this case the results will not be affected by a flat M' distribution. It worths noting that the results will be altered without the systematic errors. In this work, two cases with and without systematic errors are considered together. When the systematic errors are included, the corresponding A, B, C are expressed as

$$\begin{aligned} A &= \sum_{i,j}^{SN} \left\{5\log_{10}[\bar{d}_L(p_s, z_i)] - m_{obs}(z_i)\right\} \cdot C^{-1}_{ij} \cdot \left\{5\log_{10}[\bar{d}_L(p_s, z_j)] - m_{obs}(z_j)\right\}, \\ B &= \sum_{i}^{SN} C^{-1}_{ij} \cdot \left\{5\log_{10}[\bar{d}_L(p_s, z_j)] - m_{obs}(z_j)\right\}, \\ C &= \sum_{i}^{SN} C^{-1}_{ii}, \end{aligned} \tag{A8}$$

where C^{-1} is the inverse of covariance matrix with systematic errors. For the details and covariance matrice, one can find them in Ref. [16] and the web site [1], where one can also find the covariance matrix without systematic errors. Our form (A6) is equivalent to (A8) when C^{-1} is the inverse of covariance matrix without systematic errors.

2. Baryon Acoustic Oscillation constraints

The Baryon Acoustic Oscillations are detected in the clustering of the combined 2dFGRS and SDSS main galaxy samples, and measure the distance-redshift relation at $z = 0.2$. Additionally, Baryon Acoustic Oscillations in the clustering of the SDSS luminous red galaxies measure the distance-redshift relation at $z = 0.35$. The observed scale of the BAO calculated from these samples, as well as from the combined sample, are jointly analyzed using estimates of the correlated errors to constrain the form of the distance measure $D_V(z)$ [19–22]

$$D_V(z) = c\left(\frac{z}{\Omega_k H(z)}\mathrm{sinn}^2[\sqrt{|\Omega_k|}\int_0^z \frac{dz'}{H(z')}]\right)^{1/3}. \tag{A9}$$

The peak positions of the BAO depend on the ratio of $D_V(z)$ to the sound horizon size at the drag epoch (where baryons were released from photons) z_d, which can be obtained by using a fitting formula [23]:

$$z_d = \frac{1291(\Omega_m h^2)^{0.251}}{1 + 0.659(\Omega_m h^2)^{0.828}}[1 + b_1(\Omega_b h^2)^{b_2}], \tag{A10}$$

with

$$b_1 = 0.313(\Omega_m h^2)^{-0.419}[1 + 0.607(\Omega_m h^2)^{0.674}], \tag{A11}$$

$$b_2 = 0.238(\Omega_m h^2)^{0.223}. \tag{A12}$$

In this paper, we use the data of $r_s(z_d)/D_V(z)$, which are listed in Table III, where $r_s(z)$ is the comoving sound horizon size

$$\begin{aligned} r_s(z) &= c\int_0^t \frac{c_s dt}{a} = c\int_0^a \frac{c_s da}{a^2 H} = c\int_z^\infty dz \frac{c_s}{H(z)} \\ &= \frac{c}{\sqrt{3}}\int_0^{1/(1+z)} \frac{da}{a^2 H(a)\sqrt{1 + (3\Omega_b/(4\Omega_\gamma)a)}}, \end{aligned} \tag{A13}$$

[1] http://supernova.lbl.gov/Union/

where c_s is the sound speed of the photon−baryon fluid [24–26]:

$$c_s^{-2} = 3 + \frac{9}{4} \times \frac{\rho_b(z)}{\rho_\gamma(z)} = 3 + \frac{9}{4} \times (\frac{\Omega_b}{\Omega_\gamma})a, \tag{A14}$$

and here $\Omega_\gamma = 2.469 \times 10^{-5} h^{-2}$ for $T_{CMB} = 2.725K$.

z	$r_s(z_d)/D_V(z)$
0.2	0.1905 ± 0.0061
0.35	0.1097 ± 0.0036

TABLE III: The observational $r_s(z_d)/D_V(z)$ data [20].

Using the data of BAO in Table III and the inverse covariance matrix V^{-1} in [20]:

$$V^{-1} = \begin{pmatrix} 30124.1 & -17226.9 \\ -17226.9 & 86976.6 \end{pmatrix}. \tag{A15}$$

The radial (line-of-sight) BAO scale measurement from galaxy power spectra give constraint to cosmological parameters via the relation

$$\Delta z_{BAO}(z) = \frac{H(z) r_s(z_d)}{c} \tag{A16}$$

at two redshifts $z = 0.24$ and $z = 0.43$, the corresponding values are $\Delta z_{BAO}(z = 0.24) = 0.0407 \pm 0.0011$ and $\Delta z_{BAO}(z = 0.43) = 0.0442 \pm 0.0015$ respectively [27].

Thus, the $\chi^2_{BAO}(p_s)$ is given as

$$\chi^2_{BAO}(p_s) = X^t V^{-1} X + \frac{[\Delta z_{BAO}(z = 0.24) - 0.0407]^2}{0.0011^2} + \frac{[\Delta z_{BAO}(z = 0.43) - 0.0442]^2}{0.0015^2}, \tag{A17}$$

where X is a column vector formed from the values of theory minus the corresponding observational data, with

$$X = \begin{pmatrix} \frac{r_s(z_d)}{D_V(0.2)} - 0.1905 \\ \frac{r_s(z_d)}{D_V(0.35)} - 0.1097 \end{pmatrix}, \tag{A18}$$

and X^t denotes its transpose.

3. Cosmic Microwave Background constraints

The CMB shift parameter R is provided by [28]

$$R(z_*) = \frac{\sqrt{\Omega_m H_0^2}}{\sqrt{|\Omega_k|}} \text{sinn}[\sqrt{|\Omega_k|} \int_0^{z_*} \frac{dz'}{H(z')}], \tag{A19}$$

here, the redshift z_* (the decoupling epoch of photons) is obtained by using the fitting function [29]

$$z_* = 1048 \left[1 + 0.00124(\Omega_b h^2)^{-0.738}\right] \left[1 + g_1(\Omega_m h^2)^{g_2}\right],$$

where the functions g_1 and g_2 read

$$\begin{aligned} g_1 &= 0.0783(\Omega_b h^2)^{-0.238} \left(1 + 39.5(\Omega_b h^2)^{0.763}\right)^{-1}, \\ g_2 &= 0.560 \left(1 + 21.1(\Omega_b h^2)^{1.81}\right)^{-1}. \end{aligned}$$

In addition, the acoustic scale is related to the distance ratio and is expressed as

$$l_A = \frac{\pi}{r_s(z_*)} \frac{c}{\sqrt{|\Omega_k|}} \text{sinn}[\sqrt{|\Omega_k|} \int_0^{z_*} \frac{dz'}{H(z')}]. \tag{A20}$$

	$7-$year ML	$7-$year mean	error, σ
$l_A(z_*)$	302.09	302.69	0.76
$R(z_*)$	1.725	1.726	0.018
z_*	1091.3	1091.36	0.91

TABLE IV: The observational l_A, R, z_* data [30]. The ML values are used in this work as recommended.

Using the data of l_A, R, z_* in [30], which are listed in Table IV, and their covariance matrix of $[l_A(z_*), R(z_*), z_*]$ referring to [30]:

$$C^{-1} = \begin{pmatrix} 2.305 & 29.698 & -1.333 \\ 29.698 & 6825.270 & -113.180 \\ -1.333 & -113.180 & 3.414 \end{pmatrix}, \tag{A21}$$

we can calculate the likelihood L as $\chi^2_{CMB} = -2\ln L$:

$$\chi^2_{CMB} = \triangle d_i [C^{-1}(d_i, d_j)][\triangle d_i]^t, \tag{A22}$$

where $\triangle d_i = d_i - d_i^{data}$ is a row vector, and $d_i = (l_A, R, z_*)$.

4. Gamma Ray Bursts

Following [31], we consider the well-known Amati's $E_{p,i}-E_{iso}$ correlation [32–35] in GRBs, where $E_{p,i} = E_{p,obs}(1+z)$ is the cosmological rest-frame spectral peak energy, and E_{iso} is the isotropic energy

$$E_{iso} = 4\pi d_L^2 S_{solo}/(1+z) \tag{A23}$$

in which d_L and S_{bolo} are the luminosity distance and the bolometric fluence of the GRBs respectively. Following [31], we rewrite the Amati's relation as

$$\log\frac{E_{iso}}{\mathrm{erg}} = a + b\log\frac{E_{p,i}}{300\mathrm{keV}}. \tag{A24}$$

In [36], Wang defined a set of model-independent distance measurements $\{\bar{r}_p(z_i)\}$:

$$\bar{r}_p(z_i) \equiv \frac{r_p(z)}{r_p(z_0)}, \quad r_p(z) \equiv \frac{(1+z)^{1/2}}{z}\frac{H_0}{c}r(z), \tag{A25}$$

where $r(z) = d_L(z)/(1+z)$ is the comoving distance at redshift z, z_0 is the lowest GRBs redshift. Then, the cosmological model can be constrained by GRBs via

$$\chi^2_{GRBs}(p_s) = [\Delta\bar{r}_p(z_i)]\cdot(Cov^{-1}_{GRB})_{ij}\cdot[\Delta\bar{r}_p(z_i)], \tag{A26}$$

$$\Delta\bar{r}_p(z_i) = \bar{r}_p^{data}(z_i) - \bar{r}_p(z_i), \tag{A27}$$

where $\bar{r}_p(z_i)$ is defined by Eq. (A25) and $(Cov^{-1}_{GRB})_{ij}, i, j = 1...N$ is the covariance matrix. In this way, the constraints from amount observational GRBs data are projected into the relative few quantities $\bar{r}_p(z_i), i = 1...N$.

Following the method proposed by Wang [36], Xu obtained $N = 5$ model-independent distances data points and their covariance matrix by using 109 GRBs via Amati's $E_{p,i} - E_{iso}$ correlation [37]. The resulted model-independent distances and covariance matrix from 109 GRBs are shown below in Tab. V and Eq. (A29). The $\{\bar{r}_p(z_i)\}, i = 1, ..., 5$ correlation matrix is given by

$$(\overline{Cov}_{GRB}) = \begin{pmatrix} 1.0000 & 0.7780 & 0.8095 & 0.6777 & 0.4661 \\ 0.7780 & 1.0000 & 0.7260 & 0.6712 & 0.3880 \\ 0.8095 & 0.7260 & 1.0000 & 0.6046 & 0.5032 \\ 0.6777 & 0.6712 & 0.6046 & 1.0000 & 0.1557 \\ 0.4661 & 0.3880 & 0.5032 & 0.1557 & 1.0000 \end{pmatrix}, \tag{A28}$$

	z	$\bar{r}_p^{data}(z)$	$\sigma(\bar{r}_p(z))^+$	$\sigma(\bar{r}_p(z))^-$
0	0.0331	1.0000	–	–
1	1.0000	0.9320	0.1711	0.1720
2	2.0700	0.9180	0.1720	0.1718
3	3.0000	0.7795	0.1630	0.1629
4	4.0480	0.7652	0.1936	0.1939
5	8.1000	1.1475	0.4297	0.4389

TABLE V: Distances measured form 109 GRBs via Amati's correlation with 1σ upper and lower uncertainties [37]. $z_0 = 0.0331$ as lowest redshift was adopted.

and the covariance matrix is given by

$$(Cov_{GRB})_{ij} = \sigma(\bar{r}_p(z_i))\sigma(\bar{r}_p(z_j))(\overline{Cov}_{GRB})_{ij}, \tag{A29}$$

where

$$\sigma(\bar{r}_p(z_i)) = \sigma(\bar{r}_p(z_i))^+, \quad \text{if} \quad \bar{r}_p(z) \geq \bar{r}_p(z)^{data}; \tag{A30}$$
$$\sigma(\bar{r}_p(z_i)) = \sigma(\bar{r}_p(z_i))^-, \quad \text{if} \quad \bar{r}_p(z) < \bar{r}_p(z)^{data}, \tag{A31}$$

the $\sigma(\bar{r}_p(z_i))^+$ and $\sigma(\bar{r}_p(z_i))^-$ are the 1σ errors listed in Tab. V.

5. The X-ray gas mass fraction constraints

According to the X-ray cluster gas mass fraction observation, the baryon mass fraction in clusters of galaxies (CBF) can be utilized to constrain cosmological parameters. The X-ray gas mass fraction, f_{gas}, is defined as the ratio of the X-ray gas mass to the total mass of a cluster, which is approximately independent on the redshift for the hot ($kT \gtrsim 5keV$), dynamically relaxed clusters at the radii larger than the innermost core r_{2500}. The X-ray gas mass fraction, f_{gas}, can be derived from the observed X-ray surface brightness profile and the deprojected temperature profile of X-ray gas under the assumptions of spherical symmetry and hydrostatic equilibrium. Basing on these assumptions above, Allen et al. [13] selected 42 hot ($kT \gtrsim 5keV$), X-ray luminous, dynamically relaxed clusters for f_{gas} measurements. The stringent restriction to the selected sample can not only reduce maximally the effect of the systematic scatter in f_{gas} data, but also ensure that the f_{gas} data is independent on temperature. In the framework of the ΛCDM reference cosmology, the X-ray gas mass fraction is presented as [13]

$$f_{gas}^{\Lambda\mathrm{CDM}}(z) = \frac{KA\gamma b(z)}{1+s(z)}\left(\frac{\Omega_b}{\Omega_m}\right)\left[\frac{d_A^{\Lambda\mathrm{CDM}}(z)}{d_A(z)}\right]^{1.5}, \tag{A32}$$

where A is the angular correction factor, which is caused by the change in angle for the current test model θ_{2500} in comparison with that of the reference cosmology $\theta_{2500}^{\Lambda CDM}$:

$$A = \left(\frac{\theta_{2500}^{\Lambda\mathrm{CDM}}}{\theta_{2500}}\right)^{\eta} \approx \left(\frac{H(z)d_A(z)}{[H(z)d_A(z)]^{\Lambda\mathrm{CDM}}}\right)^{\eta}, \tag{A33}$$

here, the index η is the slope of the $f_{gas}(r/r_{2500})$ data within the radius r_{2500}, with the best-fit average value $\eta = 0.214 \pm 0.022$ [13]. And the angular diameter distance is given by

$$d_A(z) = \frac{c}{(1+z)\sqrt{|\Omega_k|}}\mathrm{sinn}[\sqrt{|\Omega_k|}\int_0^z \frac{dz'}{H(z')}], \tag{A34}$$

where $\mathrm{sinnn}(\sqrt{|\Omega_k|}x)$ respectively denotes $\sin(\sqrt{|\Omega_k|}x)$, $\sqrt{|\Omega_k|}x$, $\sinh(\sqrt{|\Omega_k|}x)$ for $\Omega_k < 0$, $\Omega_k = 0$ and $\Omega_k > 0$.

In equation (A32), the parameter γ denotes permissible departures from the assumption of hydrostatic equilibrium, due to non-thermal pressure support; the bias factor $b(z) = b_0(1+\alpha_b z)$ accounts for uncertainties in the cluster depletion factor; $s(z) = s_0(1+\alpha_s z)$ accounts for uncertainties of the baryonic mass fraction in stars and a Gaussian prior for s_0 is employed, with $s_0 = (0.16 \pm 0.05)h_{70}^{0.5}$ [13]; the factor K is used to describe the combined effects of the

residual uncertainties, such as the instrumental calibration and certain X-ray modelling issues, and a Gaussian prior for the 'calibration' factor is considered by $K = 1.0 \pm 0.1$ [13];

Following the method in Ref. [13, 38] and adopting the updated 42 observational f_{gas} data in Ref. [13], the best fit values of the model parameters for the X-ray gas mass fraction analysis are determined by minimizing,

$$\chi^2_{CBF} = \sum_i^N \frac{[f_{gas}^{\Lambda\mathrm{CDM}}(z_i) - f_{gas}(z_i)]^2}{\sigma^2_{f_{gas}}(z_i)}, \tag{A35}$$

where $\sigma_{f_{gas}}(z_i)$ is the statistical uncertainties (Table 3 of [13]). As pointed out in [13], the acquiescent systematic uncertainties have been considered according to the parameters i.e. $\eta, b(z), s(z)$ and K.

6. Lookback Time

Since the seminal work of Sandage [39] who defines the lookback time as the difference between the present age of the Universe (t_0) and its age (t_z) when a particular light ray at redshift z was emitted, one has used the lookback time-redshift relation to constrain cosmological models, for example lookback time as a constraint to DGP model [40]. The lookback time-redshift relation is given by

$$t_L(z) = \int_0^z \frac{dz'}{(1+z')H(z')}. \tag{A36}$$

Following Capozziello et al. [41], one can define the age $t(z_i)$ of an object (e.g., a galaxy, a quasar or a galaxy cluster) at redshift z_i as the difference between the age of the Universe at z_i and the age z_F when the object was born,

$$\begin{aligned} t(z_i) &= \int_{z_i}^{\infty} \frac{dz'}{(1+z')H(z')} - \int_{z_F}^{\infty} \frac{dz'}{(1+z')H(z')} \\ &= t_L(z_F) - t_L(z_i). \end{aligned} \tag{A37}$$

Then the observed lookback time to an object at z_i can be defined as

$$\begin{aligned} t_L^{obs}(z_i) &= t_L(z_F) - t(z_i) = [t_0^{obs} - t(z_i)] - [t_0^{obs} - t_L(z_F)] \\ &= t_0^{obs} - t(z_i) - df, \end{aligned} \tag{A38}$$

where df is the delay factor which accounts for our ignorance about the absolute age of universe when the object is formed at $t(z_F)$. To constrain a cosmological model by using lookback time of an object, one can use

$$\chi^2_{age} = \sum_i \frac{[t_L(z_i) - t_L^{obs}(z_i, df)]^2}{\sigma_T^2} + \frac{[t_0 - t_0^{obs}]^2}{\sigma^2_{t_0^{obs}}} \tag{A39}$$

where $\sigma_T^2 = \sigma_i^2 + \sigma^2_{t_0^{obs}}$, σ_i is the uncertainty of the individual lookback time to the i^{th} galaxy of our sample and $\sigma_{t_0^{obs}}$ is the uncertainty on the total expansion age of the universe. After marginalizing the 'nuisance' parameter df, one can use the following method to constrain a cosmological model by using lookback time [42]

$$\begin{aligned} \chi^2_{LT}(p_s) &= -2\ln \int_0^{\infty} d(df) \exp(-\chi^2_{age}/2) \\ &= A - \frac{B^2}{C} + D - 2\ln[\sqrt{\frac{\pi}{2C}}\mathrm{erfc}(\frac{B}{\sqrt{2C}})], \end{aligned} \tag{A40}$$

where

$$A = \sum_i \frac{\Delta^2}{\sigma_T^2}, \quad B = \sum_i \frac{\Delta}{\sigma_T^2}, \quad C = \sum_i \frac{1}{\sigma_T^2}, \tag{A41}$$

where Δ is

$$\Delta = t_L(z_i) - [t_0^{obs} - t(z_i)] \tag{A42}$$

and D is the second term of Eq. (A39), $\mathrm{erfc}(x) = 1 - \mathrm{erf(x)}$ is the complementary error function of the variable x. The observational data points of the age of galaxies are shown in Tab. VI . The current observational universe age is $t_0^{obs} = 13.75 \pm 0.13$Gyr [30].

z_i	$t_i(z_i)$ (Gyr)
0.1171	10.2
0.1174	10.0
0.2220	9.0
0.2311	9.0
0.3559	7.6
0.4520	6.8
0.5750	7.0
0.6440	6.0
0.6760	6.0
0.8330	6.0
0.8360	5.8
0.9220	5.5
1.179	4.6
1.222	3.5
1.224	4.3
1.225	3.5
1.226	3.5
1.340	3.4
1.380	3.5
1.383	3.5
1.396	3.6
1.430	3.2
1.450	3.2
1.488	3.0
1.490	3.6
1.493	3.2
1.510	2.8
1.550	3.0
1.576	2.5
1.642	3.0
1.725	2.6
1.845	2.5
0.60	9.20
0.70	9.80
0.80	3.41
0.10	3.08
0.25	4.84
1.27	12.13

TABLE VI: Galaxy ages **(author?)** [43]. The last 6 data points are taken from the Capozziello et al. [41] (Table 1) ages of 6 galaxy clusters in the redshift range $0.10 < z < 1.27$. The 1σ error are taken as 12% of the age of galaxy with exception of the last 6 data points. The 1σ error of the last 6 data points are set as 1.

7. Growth Function of Matter Linear Perturbations

The linear growth factor of the matter density perturbation $D(a)$ is defined as

$$D(a) \equiv \frac{\frac{\delta\rho}{\rho}(a)}{\frac{\delta\rho}{\rho}(a=1)}, \tag{A43}$$

which is subject to the evolution equation [38, 44]

$$D^{''}(k,a)+\left(\frac{3}{a}+\frac{E'(a)}{E(a)}\right)D^{'}(k,a)-\frac{3}{2}\frac{\Omega_{m0}}{a^5E(a)}f(k,a)D(k,a)=0 \tag{A44}$$

with initial conditions $D(a)\simeq a$ for $a\simeq 0$ on sub-Hubble scales, where $'$ denotes derivative with respect to scale factor a and $E(a)=H(a)/H_0$. The forms of $f(k,a)$ depend on the dynamical equations of particular gravity theory. For general relativity, $f(k,a)\equiv 1$. For the case of DGP model, $f(k,a)$ takes the form

$$f(k,a)=(1+\frac{1}{3\alpha}), \tag{A45}$$

where α is

$$\alpha=1-\frac{E(a)}{\sqrt{\Omega_{r_c}}}\left(1+\frac{a}{3}\frac{E'(a)}{E(a)}\right). \tag{A46}$$

The observational growth rate relates to $D(a)$ via

$$g(a)\equiv\frac{aD'(a)}{D(a)}=\frac{d\ln\delta}{d\ln a}. \tag{A47}$$

The current data sets about growth function are listed in Tab. VII.

z_i	g_i^{obs}	Reference
0.15	0.51 ± 0.11	[45]
0.35	0.70 ± 0.18	[46]
0.55	0.75 ± 0.18	[47]
0.77	0.91 ± 0.36	[48]
1.4	0.90 ± 0.24	[49]
3.0	1.46 ± 0.29	[50]

TABLE VII: Observed perturbation growth as a function of redshift z, where $g(a)=\frac{d\ln\delta}{d\ln a}$ in terms of a.

Then, the constraint from growth function is in the form

$$\chi^2_{GF}(p_s)=\sum_i\left[\frac{g(z_i)-g_i^{obs}}{\sigma_i}\right]^2. \tag{A48}$$

[1] A. G. Riess *et al.*, Astron. J. **116** 1009 (1998) [astro-ph/9805201].
[2] S. Perlmutter *et al.*, Astrophys. J. **517** 565 (1999) [astro-ph/9812133].
[3] S. Weinberg, *The cosmological constant problem,* Rev. Mod. Phys. **61**, 1 (1989); V. Sahni and A. A. Starobinsky, *The Case for a Positive Cosmological Lambda-term,* Int. J. Mod. Phys. D **9**, 373 (2000) [arXiv:astro-ph/9904398]; S. M. Carroll, *The cosmological constant,* Living Rev. Rel. **4**, 1 (2001) [arXiv:astro-ph/0004075]; P. J. E. Peebles and B. Ratra, *The cosmological constant and dark energy,* Rev. Mod. Phys. **75**, 559 (2003) [arXiv:astro-ph/0207347]; T. Padmanabhan, *Cosmological constant: The weight of the vacuum,* Phys. Rept. **380**, 235 (2003) [arXiv:hep-th/0212290]; E. J. Copeland, M. Sami and S. Tsujikawa, *Dynamics of dark energy,* Int. J. Mod. Phys. D **15**, 1753 (2006) [arXiv:hep-th/0603057].
[4] G. R. Dvali, G. Gabadadze, M. Porrati, Phys. Lett. B. 485, 208(2000) [arXiv:hep-th/0005016].
[5] A. Lue, Phys. Rept. 423, 1(2006) [arXiv:astro-ph/0510068].
[6] M. Li, X. Li, X. Zhang, arXiv:0912.3988v1[astro-ph.CO].
[7] H. Zhang, H. Yu, H. Noh, Z. Zhu, Phys. Lett. B 665, 319(2008) arXiv:0806.4082v2[astro-ph].
[8] L. Lombriser, W. Hu, W. Fang, U. Seljak, Phys. Rev. D 80,063536(2009).
[9] H. Wei, Phys. Lett. B 664,1(2008) arXiv:0802.4122v3 [astro-ph].
[10] S. Nesseris and L. Perivolaropoulos, Phys. Rev. D 77, 023504 (2008) [arXiv:0710.1092].
[11] C. Deffayet et al., Phys. Rev. D 66, 024019 (2002).
[12] A. Lewis and S. Bridle, Phys. Rev. D **66** 103511 (2002); URL: http://cosmologist.info/cosmomc/.

[13] S. W. Allen, D. A. Rapetti, R. W. Schmidt, H. Ebeling, R. G. Morris and A. C. Fabian, Mon. Not. Roy. Astron. Soc. **383** 879 (2008).
[14] D. Rapetti, S. W. Allen and J. Weller, Mon. Not. Roy. Astron. Soc. **360** 555 (2005).
[15] URL: http://www.stanford.edu/∼drapetti/fgas_module/
[16] R. Amanullah et al. [Supernova Cosmology Project Collaboration], arXiv:1004.1711 [astro-ph.CO].
[17] S. Nesseris and L. Perivolaropoulos, Phys. Rev. D **72** 123519 (2005); L. Perivolaropoulos, Phys. Rev. D **71** 063503 (2005); E. Di Pietro and J. F. Claeskens, Mon. Not. Roy. Astron. Soc. **341** 1299 (2003); A. C. C. Guimaraes, J. V. Cunha and J. A. S. Lima, JCAP **0910** 010 (2009).
[18] E. Garcia-Berro, E. Gaztanaga, J. Isern, O. Benvenuto and L. Althaus, astro-ph/9907440; A. Riazuelo and J. Uzan, Phys. Rev. D **66** 023525 (2002); V. Acquaviva and L. Verde, JCAP **0712** 001 (2007).
[19] T. Okumura, T. Matsubara, D. J. Eisenstein, I. Kayo, C. Hikage, A. S. Szalay and D. P. Schneider, Astrophys. J. **676** 889 (2008).
[20] W. J. Percival *et al.*, arXiv:0907.1660 [astro-ph.CO].
[21] D. J. Eisenstein *et al.*, [SDSS Collabaration], Astrophys. J. **633** 560 (2005) [astro-ph/0501171].
[22] W. J. Percival *et al.*, Mon. Not. R. Astron. Soc. **381** 1053 (2007) arXiv:0705.3323 [astro-ph.CO].
[23] D. J. Eisenstein and W. Hu, Astrophys. J. **496** 605 (1998).
[24] W. Hu and N. Sugiyama, Astrophys. J. **444** 489 (1995) [arXiv:astro-ph/9407093].
[25] W. Hu, M. Fukugita, M. Zaldarriaga and M. Tegmark, Astrophys. J. **549** 669 (2001) [arXiv:astro-ph/0006436].
[26] R. R. Caldwell and M. Doran, Phys. Rev. D **69** 103517 (2004).
[27] E. Gaztanaga, R. Miquel, E. Sanchez, Phys. Rev. Lett. 103 091302(2009).
[28] J. R. Bond, G. Efstathiou and M. Tegmark, Mon. Not. Roy. Astron. Soc. **291** L33 (1997).
[29] W. Hu and N. Sugiyama, Astrophys. J. **471** 542 (1996).
[30] E. Komatsu et al. [WMAP Collaboration], arXiv:1001.4538 [astro-ph.CO].
[31] B. E. Schaefer, Astrophys. J. 660, 16 (2007) [astro-ph/0612285].
[32] L. Amati et al., Astron. Astrophys. 390, 81 (2002) [astro-ph/0205230].
[33] L. Amati *et al.*, Mon. Not. Roy. Astron. Soc. **391**, 577 (2008) [arXiv:0805.0377].
[34] L. Amati, arXiv:1002.2232 [astro-ph.HE]; L. Amati, Mon. Not. Roy. Astron. Soc. 372, 233 (2006) [astro-ph/0601553].
[35] L. Amati, F. Frontera and C. Guidorzi, arXiv:0907.0384 [astro-ph.HE].
[36] Y. Wang, Phys.Rev.D 78,123532(2008).
[37] L. Xu, arXiv:1005.5055v1 [astro-ph.CO].
[38] S. Nesseris and L. Perivolaropoulos, JCAP **0701** 018 (2007) [astro-ph/0610092].
[39] A. Sandage, Annu. Rev. Astron. Astrophys. 26, 561 (1988).
[40] N. Pires, Z. Zhu, J. S. Alcaniz, Phys.Rev.D 73, 123530 (2006).
[41] S. Capozziello, V. F. Cardone, M. Funaro, and S. Andreon, Phys. Rev. D 70, 123501 (2004).
[42] M. A. Dantas, J. S. Alcaniz, D. Jain, A.Dev, Astron. Astrophys. 467 (2007) 421.
[43] Simon, J., Verde, L., & Jimenez, R. 2005, Phys. Rev. D, 71, 123001.
[44] J. P. Uzan, Gen.Rel.Grav.39,307(2007) [arXiv:astro-ph/0605313v1]; H. F. Stabenau, B. Jain, Phys.Rev. D74, 084007(2006) [arXiv:astro-ph/0604038v3].
[45] E. Hawkins *et al.*, Mon. Not. Roy. Astron. Soc. **346**, 78 (2003) [astro-ph/0212375];
L. Verde *et al.*, Mon. Not. Roy. Astron. Soc. **335**, 432 (2002) [astro-ph/0112161];
E. V. Linder, arXiv:0709.1113 [astro-ph].
[46] M. Tegmark *et al.* [SDSS Collaboration], Phys. Rev. D **74**, 123507 (2006) [astro-ph/0608632].
[47] N. P. Ross *et al.*, astro-ph/0612400.
[48] L. Guzzo *et al.*, Nature **451**, 541 (2008) [arXiv:0802.1944].
[49] J. da Angela *et al.*, astro-ph/0612401.
[50] P. McDonald *et al.* [SDSS Collaboration], Astrophys. J. **635**, 761 (2005) [astro-ph/0407377].